Wind Turbine Emulator for Wind Power Generation System

N. Suppaadirek, S. Ruengkittrakarn, and S. Tammaruckwattana
School of Engineering King Mongkut's Institute of Technology Ladkrabang, Bangkok, Thailand
Email: {62601186; 59601027; sirichai.ta}@kmitl.ac.th

***Abstract*—This paper proposes the wind turbine emulator for wind power generation systems. The focus is on simulation of the operation of wind turbines at different wind speeds to test the capacity and efficiency of generating three-phase electricity. The wind turbine emulator consists of a simulation program and a mechanical part. To simulate the power generation system of wind turbines, researchers use a 400-watt permanent magnet synchronous generator wind turbine connected to a 400-watt servo motor with a built-in absolute encoder and controlled by a servo driver. The motor's torque is controlled by data from mathematical equations in the MATLAB model.**

***Index Terms*—Mechanical model, permanent magnet synchronous generator, wind energy, wind turbine emulator**

I. Introduction

Nowadays the demand for electric power is increasing day by day. The electricity used today is derived from natural gas produced from coal, produced by the water pressure in the dam, and renewable energy such as biomass energy, solar energy, and wind energy. It is well known that fossil fuels are a finite resource. It took a long time to build, and this type of fuel is expected to run out in the future. By then, renewable energy will play a more significant role and could become a primary energy source in the future [1]. Renewable energy is an alternative form of energy that is clean, highly efficient, easy to find, and environmentally friendly [2]-[5]. Wind power is natural energy generated by temperature differences, atmospheric pressure, and the earth's rotational forces. These are the factors that contribute to wind speed and wind power. Wind energy, like solar energy, is not a costly resource. Currently, wind energy has been utilized more and more [6]. There are devices that help in converting wind energy into other forms of energy, such as wind turbines that turn wind power into electrical energy.

Renewable energy of wind turbine systems is mainly based on permanent magnet synchronous generator (PMSG) and double fed induction generator (DFIG) [7]. The wind turbine with PMSG is more reliable than DFIG because the PMSG system does not require a gear system [8]. It can be installed in almost any terrain and generate electricity if there is wind. Wind turbines are designed to handle various wind speeds because the wind speed is not the same, even in areas not very far from each other. The speed of the wind is directly proportional to the rotation of the wind turbine blades.

In this paper, the researchers focus on developing a wind turbine emulator system at various wind speeds to test the ability and efficiency of various types of wind turbine blades. Therefore, the study focuses on wind turbines with permanent magnet pole generator systems and permanent magnet generator wind turbine operating systems.

Wind turbine emulators can be divided into three groups. Electrical-mechanical simulations, program-based simulations, and power electronic simulations [9]-[11]. The most common wind turbine system simulation is the electrical-mechanical, which consists of a generator in conjunction with a motor. On the motor side, it can be used with a DC motor [12], an induction motor with a speed drive control, an induction motor with frequency control [13], or an induction motor with torque control depending on their control system [14]-[16]. The generator side can use either a three-phase synchronous generator [17], a permanent magnet synchronous generator (PMSG) [18]-[22], or a DC motor. The researchers choose a simulated electrical machines method and control the operation using a computer program.

This paper describes the experimental verification of electrical-mechanical simulations conducted with an AC servo motor attached to the PMSG wind turbine shaft. The program part is made in MATLAB/Simulink, which contains several calculations blocks necessary for creating wind turbine behavior [23].

The wind turbine model is based on the blade element momentum theory proposed in [24]. The proposed model was constructed with fluid analysis considering the wing shapes of the wind turbine.

II. Wind Turbine Emulator

Fig. 1 shows the basic structure of a wind turbine emulator system. This research used Blade Element Momentum Theory (BEM) to model wind turbines. The wind turbine model contains three-dimensional data of the wind turbine characteristics used to generate the

Manuscript received October 25, 2021; revised December 10, 2021; accepted December 20, 2021.
Corresponding author: S. Tammaruckwattana (email: sirichai.ta@kmitl.ac.th).

doi: 10.18178/ijeetc.11.3.226-233

behavior of the wind turbine blades when in contact with natural wind, as well as a mechanical model showing the difference between an actual wind turbine and a simulated wind turbine driven by a motor drive. The wind turbine model is the core of the simulation, as we did not use an actual wind turbine or wind blade in this research to generate the torque needed to drive the generator. The wind speed is the default variable for the simulator. The rotational speed is generated by the encoder (RE) attached to the motor. The wind speed was specified as the first condition of the simulator. The wind speed has a variable value and contains sinusoidal values of the intention to replicate actual wind speed, which can change from time to time.

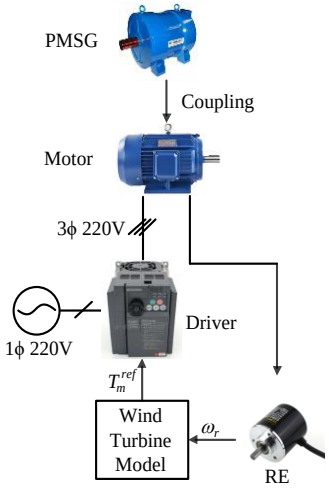

Fig. 1. Wind turbine emulator structure.

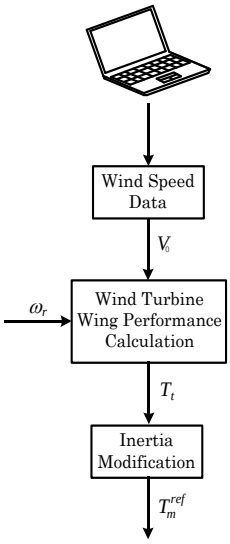

Fig. 2. Wind turbine model and inertia model.

Fig. 2 shows the workflow of the wind turbine emulator system, where the data transmission and calculations come from mathematical equation blocks generated by the MATLAB/Simulink program. The value of the signal to be fed into the driver operating system must be referenced from the equations data set. The functional diagram can be illustrated as follows. The illustration of the computer in Fig. 2 represents the data that has been put in the system as an input or parameter. The concept of the wind turbine simulator system looks similar to [25] in terms of the input data and torque reference but different in motor and program logic since this research uses servo motor with driver instead of DC motor.

A. Wind Speed Data

The first part of the wind turbine model shown in Fig. 2 is wind speed data. Wind speed data is a set of instructions for generating wind speed signals. The speed value depends on the size of the signal inserted into the block.

B. Wind Turbine Wing Performance Calculation

The wind turbine power calculation is a set of instructions created by simulating the wind flows through the turbine blades. Kinetic energy is transferred to the blades, causing the turbine to rotate around its axis and generate mechanical energy or torque (T_t) in the system. The resulting value varies depending on the type and size of the turbine blades. Various information is calculated from the BEM data of the turbine blades simulated from the fluid program obtained from wind shape in Table I, a previous research work by researchers [24]. The airfoil structure is shown in Fig. 3. The main values used are the lift coefficient C_l and drag coefficient C_d. The three-dimensional data are calculated by applying the lift coefficient C_l and drag coefficient C_d obtained by fluid analysis into the equation of blade momentum theory.

Table I shows the wing blade parameter made from NACA4412 [24].

The cross-section of blade shape is shown in Fig. 4. The xu, yu coordinate is the upper part of the airfoil, and the xl, yl coordinates are the lower part.

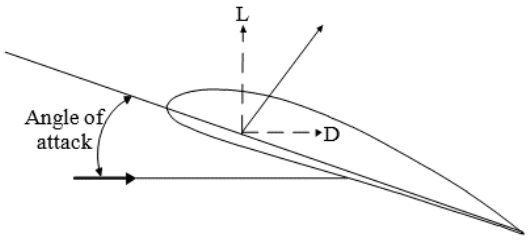

Fig. 3. Lift and drag.

TABLE I: WING SHAPE

Code number	R[m] distance from the center of the rotor	C[m] width of code	β[deg] angle of twist
1	0.08	0.096	-
2	0.10	0.094	-
3	0.12	0.093	-
4	0.14	0.092	1.5
5	0.16	0.090	3.2
6	0.21	0.085	4.5
7	0.41	0.066	4.8
8	0.61	0.048	4.9
9	0.66	0.044	4.9
10	0.71	0.040	5
11	0.76	0.035	5

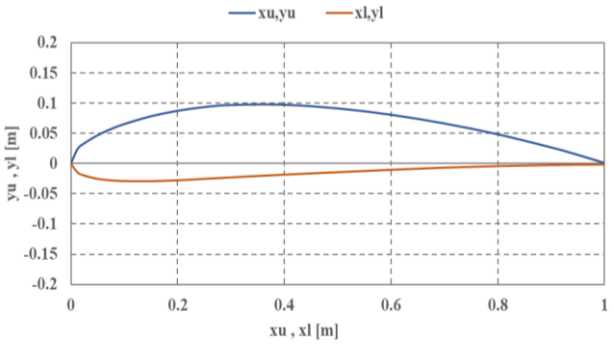

Fig. 4. Coordinate data of naca4412.

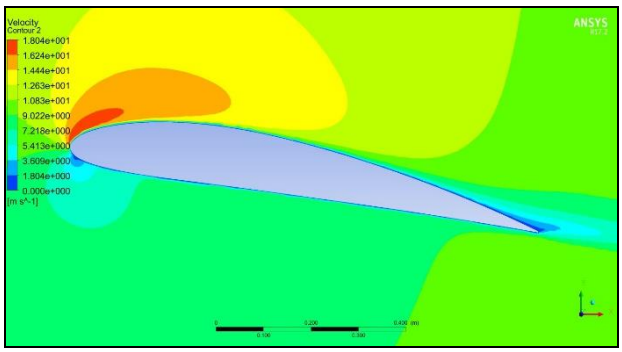

Fig. 5. The angle of attack of 10 [deg] of the wind velocity distribution.

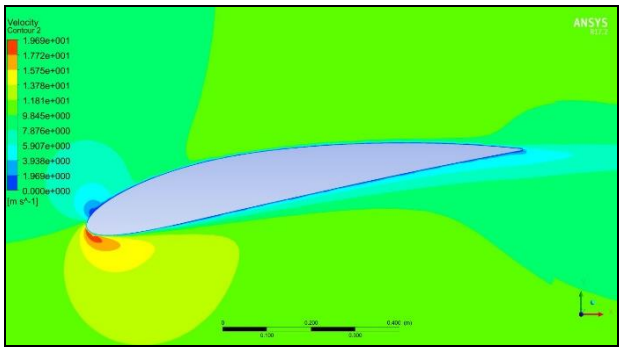

Fig. 6. The angle of attack of 10 of the wind velocity distribution.

ANSYS Fluent uses the XY coordinate data. Fig. 5 and Fig. 6 show the examples of data simulators depicting the wind speed distribution for the NACA4412 profile at a meeting angle of 10° and −10°. C_l and C_d are calculated from the lift L and drag D obtained from Fluent from (1)

$$c_l = \frac{2L}{\rho V_0^2 c}, \quad c_d = \frac{2D}{\rho V_0^2 c} \tag{1}$$

where ρ is the air density [kg/m^3], L represents the lift, D represents drag, V_0 is the wind velocity [m/s], and c is the width of code.

C. Inertia Modification

The next part of the wind turbine emulator is the inertia modification. This section contains real wind turbine systems and wind turbine simulators [26]-[28].

Fig. 7 (a) shows the mechanical system of the actual wind turbine. The torque and speed of the wind turbine come from the rotation of the rotor and are then transmitted to generator torque and rotational speed through the gearbox. The mechanical system of an actual wind turbine is described as follows:

$$\left\{ J_g + J_t \left(\frac{n_2}{n_1} \right)^2 \right\} \frac{d\omega_g}{dt} = T_g - T_t \frac{n_2}{n_1} - \left\{ B_g + B_t \left(\frac{n_2}{n_1} \right)^2 \right\} \omega_g \tag{2}$$

where T_t is the wind turbine torque [Nm], T_g is the generator torque [Nm], J_t is the wind turbine moment of inertia [kgm^2], J_g is the generator moment of inertia [kgm^2], B_t is the wind turbine coefficient of viscosity [Nm/(rad/s)], B_g is the generator coefficient of viscosity [Nm/(rad/s)], ω_g is the generator rotational speed, and n_2/n_1 is the gear ratio.

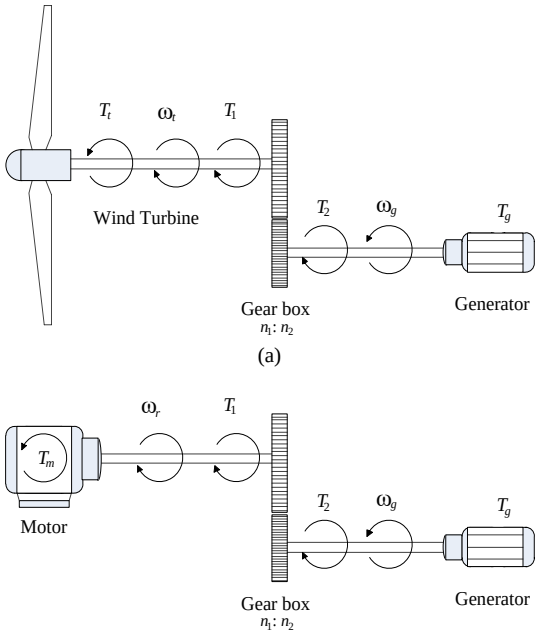

Fig. 7. (a) Real turbine and (b) Motor model.

Fig. 7 (b) shows the mechanical system of the wind turbine emulator, which consists of a motor. The motor torque and speed come from the rotation of the motor and are then transmitted to generator torque and rotational speed through a gearbox. The mechanical systems of wind turbine emulators are described as follows:

$$\left\{ J_g + J_m \left(\frac{n_2}{n_1} \right)^2 \right\} \frac{d\omega_g}{dt} = T_g - T_m \frac{n_2}{n_1} - \left\{ B_g + B_m \left(\frac{n_2}{n_1} \right)^2 \right\} \omega_g . \tag{3}$$

where J_m is the induction motor moment of inertia [kgm^2], T_m is the motor torque [Nm], and B_m is the motor coefficient of viscosity [Nm/(rad/s)].

Inertial modification is a series of mathematical calculations to convert wind turbine system to motor system because, in this research, the servo motor is used to drive the generator, not an actual wind turbine. Therefore, it is necessary to relate the torque T_t generated by the turbine blade to the torque T_m generated by the motor. The torque control and inertia modification are also used in [29], with a squirrel cage induction motor as the drive source. Since the stator of the induction motor consists of coils while the stator of the servo motor consists of a permanent magnet, the inertia of the induction motor is very high while the inertia of the servo

motor is low. For this reason, a servo motor can be stopped very quickly. A servo motor is more effective than an induction motor when high torque, positioning, and brake control are required. The difference between T_t and T_m can be compensated by

$$T_m^{ref} = \frac{J_m}{J_t}\left(T_t - B_t\omega_t\right) + B_m\omega_t \,. \quad (4)$$

where T_m^{ref} is the induction motor torque reference [Nm], and ω_t is the wind turbine emulator rotational speed.

D. Controller

When the motor's torque has been acquired, the next step is to send the data to the driver, as shown in Fig. 1. The driver used in this research requires an analog input as a torque command for torque control. Therefore, the microcontroller used in this research must receive data from MATLAB and forward the analog data to the controller driver. The microcontroller chosen for this research is the Arduino Due Board. It is one of the few Arduino boards equipped with two real DAC converter channels and has high processing power (ARM Cortex-M3 core), which improves the execution speed of the digital controller [30]-[31]. In some projects related to wind turbines, the Arduino board has been used as a microcontroller in data acquisition and processing systems [32]-[33]. In [34], a control system was presented using FPGA with MATLAB to control a DC motor. FPGA is more expensive and complex than Arduino.

The data received from the inertial block needs to be converted into a data set that the microcontroller can understand. Therefore, an additional MALAB block in the wind turbine acts as a data conversion system. The hardware also had to be modified because the input and output ranges of the Arduino Due and the driver did not match. The microcontroller board has an operating voltage of 3.3 V. This means that the maximum voltage that the DAC can produce is 3.3 V. In contrast, the driver's analog input commands for speed and torque are 10 V and 9 V, respectively. Conditioning hardware had to be developed to connect the Arduino Due Board to the driver system. Therefore, the system requires control circuitry to adjust the D/A output signal. The chosen microcontroller, control circuit inspiration, and MATLAB control method for the Arduino were explained in [35]. The microcontroller also receives the pulse data from the encoder through the driver. Programming in the Arduino is also required to convert the pulse data into rotational speed [rpm] data [36]. The control system in [37] also uses the MATLAB control method, but with a PI controller and fuzzy logic with a DC motor as the drive, which requires more computational effort than controlling the servo motor used in this research. The Arduino system supports C++, but other languages can be used with the appropriate software [38].

III. Experimental System

When the wind turbine emulator system is integrated with the device and external circuits, it can be described in Fig. 8. A microcontroller controls this system. The wind turbine model uses wind data as input to generate torque reference. The velocity data is input through the data stored on the computer, and the angular velocity is obtained from the encoder through the microcontroller. The driver controls the motor torque. The motor operates based on the reference torque value provided by the microcontroller. The encoder sends the signal back to MATLAB/Simulink [39] through the bifurcation circuit, a filter for the encoder when the motor rotates. The torque output is convergent to T_m^{ref} .

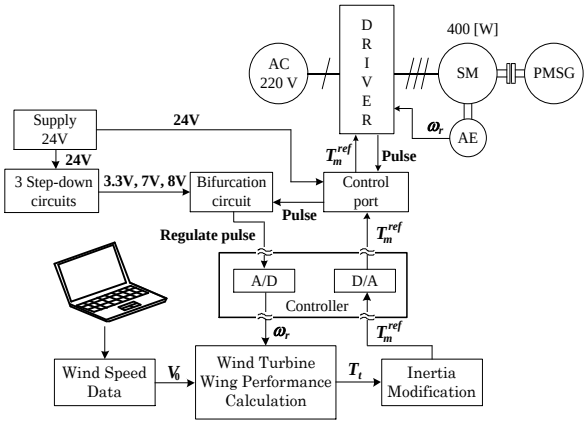

Fig. 8. Experimental system.

Fig. 9 shows the change in wind speed, V_0 [m/s]. The 140s is the simulation time used for the simulation process. The change in wind speed includes the ranges of low wind speed of 5 m/s, which increases to 6 m/s at the 70s, and then changes to the range of medium wind speed of 7 m/s at 95s. At the high wind speed of 9.2 m/s at 132s, there is turbulence in the wind speed at the 50s, 75s, and 100s made to duplicate the sudden change in wind speed. The turbulence is used to test the performance of the wind turbine emulation system and whether the system can work in the actual wind, which is not a stable value. Moreover, the wind speed increase was represented as a slope to duplicate the actual wind speed, which keeps increasing with time.

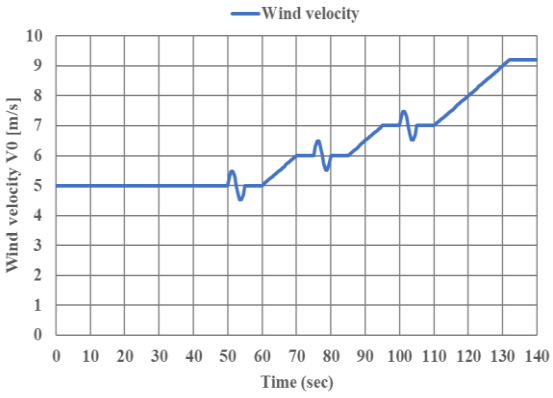

Fig. 9. Wind velocity.

Fig. 10 shows the difference between the experimental wind turbine torque and the simulated wind turbine torque calculated using the wind turbine model block. The simulation time is 140s. The simulation data is from mathematical calculations, while the experimental data is

from the actual motor. At 0s to 12s, the wind turbine simulation graph shows that the wind turbine does not start properly. At 0s to 5s, the experimental graph for the wind turbine torque is also uncontrollable. After 12s, the system starts to control, and two values approach 0.6 N/m, which means that the experimental system worked correctly. When the input velocity became sinusoidal, the experimental value was slightly unstable but still under control. The highest value is 0.8 N/m, while the lowest is 0.3 N/m for the simulation data. In the 60s to 70s, the torque increases from 0.6 to 0.8 N/m. At 75s, the system experiences another sinusoidal signal, shifting the torque signal between 1 and 0.38 N/m for the simulation data. The experimental value was slightly unstable but still within control. At 85s to 95s, the torque increases from 0.7 to 0.8 N/m. The experimental data still follows the simulation value but is less stable than a constant simulation. At 75s, the system experiences another sinusoidal signal that causes a shift in the torque signal between 1 and 0.9 N/m. The experimental value is still under control. After 95s, the sinusoidal signal causes the simulation torque signal to move between 1.1 and 0.5 N/m. The torque experiment still follows the simulation. When the system enters the high-speed range at 120s to 140s, the experimental value increases and decreases rapidly, which means that the control system is less efficient in the high-speed range, but it is still controllable because the value continuously approaches the simulation value.

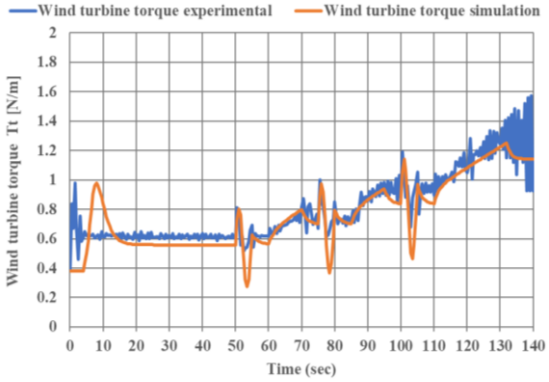

Fig. 10. Wind turbine torque experimental and Wind turbine toque simulation.

Fig. 11 shows the difference in value between the wind turbine torque simulation and the motor torque simulation resulting from the inertia modification block. The simulation time is 140s. The y-axis of these two values is different due to the conversion from the actual wind turbine torque simulation to the motor torque simulation, which is used as the control signal data sent to the microcontroller to control the motor. The y-axis on the left side of the diagram is the wind turbine torque simulation, while the right is the motor torque simulation. The wind turbine torque simulation graph is the same as in Fig. 10. The shape of the graph looks identical, but the value is different. At 0s to 12s, the graph shows that the wind turbine does not start properly, resulting in a sudden shift of the value from 0.4 to 1 N/m in the wind turbine torque simulation and from 0.03 to 0.08 N/m in the motor torque simulation.

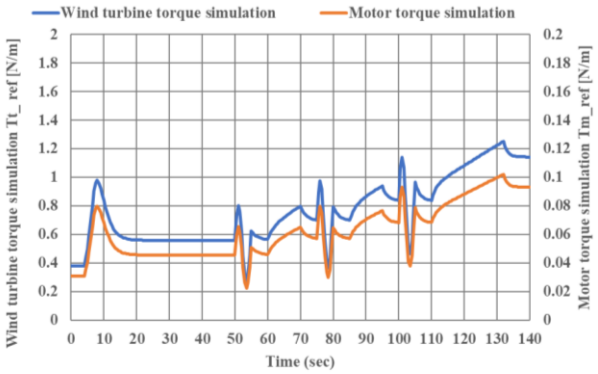

Fig. 11. Wind turbine torque simulation and Motor toque simulation.

Fig. 12 shows the difference between the experimental wind turbine torque and the experimental motor torque calculated from the inertia modification block. The y-axis of these two values is different from that in Fig. 11. The y-axis on the left side of the plot is the experimental wind turbine torque, while the right side is the experimental motor torque. The experimental wind turbine torque graph is the same as in Fig. 10. The shape of the graph looks identical, but the value is different. The graph shows that the experimental value has some ripple due to the actual motor performance. At 0-5s, the graph shows that the wind turbine system does not start properly, resulting in a sudden shift of the value from 0.5 to 1 N/m in the wind turbine torque simulation and from 0.04 to 0.08 N/m in the motor torque simulation. At the 120s, when the system enters the high wind zone, there is more ripple data than the low and medium wind speed zone.

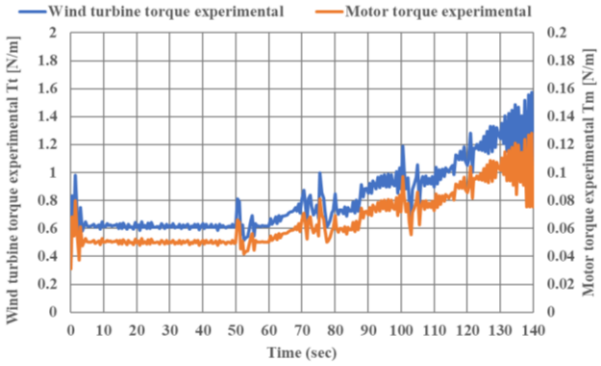

Fig. 12. Wind turbine torque experimental and Motor toque experimental.

Fig. 13 shows the difference between the simulated and experimental motor torque. Both data are from the right side of the y-axis in Figs. 11 and 12, which are calculated from the inertia modification block. This figure explains the control situation of the wind turbine emulator system when the wind turbine model data is converted to the inertia modification block in the simulation and experimental perspective. Since the data itself is from the wind turbine torque, it also inherited the control situation of wind turbine torque experimental compared with wind turbine torque simulation in Fig. 10. The behavior of the experimental diagram differs from that of the simulated diagram, as the control system for the simulation only starts control after 12s, while the experimental diagram reaches control after 5s.

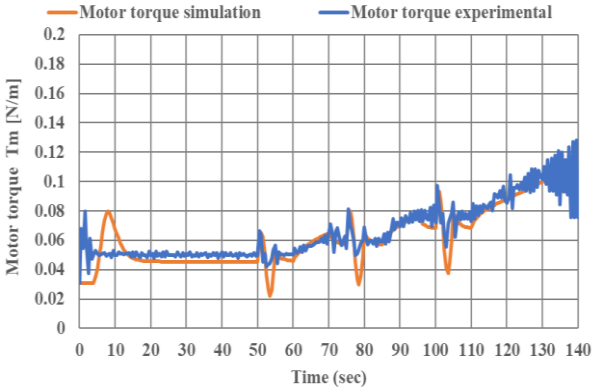

Fig. 13. Motor torque simulator and Motor toque experimental.

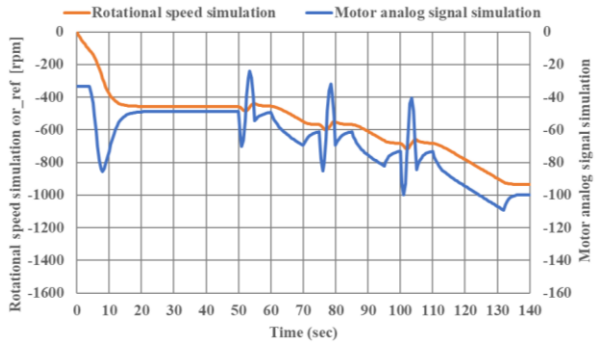

Fig. 14. Rotational speed simulation and Motor analog signal simulation.

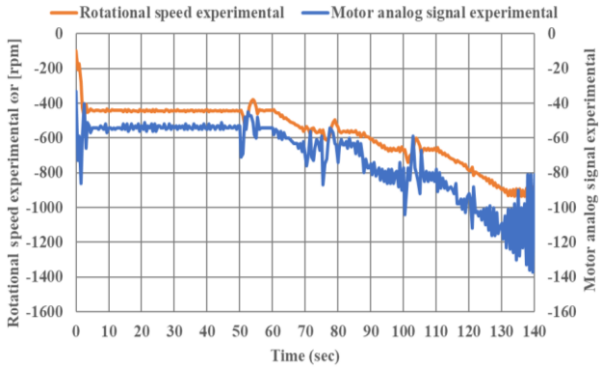

Fig. 15. Rotational speed experimental and motor analog signal experimental.

Fig. 14 shows the rotational speed simulation compared to the simulation of the analog motor signal converted from the torque output simulation. The y-axis of these two values is different. The y-axis on the left represents the rotation speed simulation, and the one on the right represents the analog motor signal simulation. At 0s to 12s, the graph shows that the wind turbine is not starting correctly, causing the value of the analog motor signal to increase to 80 suddenly. After 12s, the system starts to regulate, and the shape of the graph looks slightly identical.

Fig. 15 shows the rotational speed experiment compared to an analog signal experiment converted from the experimental torque output. The y-axis of these two values is different. The y-axis on the left side is the experimental velocity, and the right side is the experimental analog signal from the motor. The graph shows that the experimental value has some ripple due to the actual motor output and the stability of the microcontroller signal. The motor signal also has a high ripple when it enters a high wind speed area. Since the microcontroller can only receive digital data, the system must convert analog data to digital data. The microcontroller then converts this signal back to analog values to control the motor through a driver that uses the analog signal as reference data. The process involves electrical circuitry to amplify the signal required for use as a reference signal, as the microcontroller does not have an acceptable signal range to control the motor at maximum speed.

Fig. 16 shows the comparison between the rotational speed simulation and the rotational speed experiment. For wind turbine emulation systems using accurate engine data, deviations from the reference values obtained from the simulation data system occur during the first 0 to 12 seconds of operation, so the plots are quite different. After the 12 second period, when the data is high and stable enough, the motor starts to regulate correctly, causing the data in the encoder circuit to become turbulent and the data to deviate a little from the real-time speed, but still closer to the simulation value than in the first 12 seconds. At the 60s, the simulation value increases as a slope from 420 rpm to 580 rpm. The experimental data still follows the simulation but does not have the same performance as when the simulation value is stable. At 85, the rotation speed increases steeply again. The performance is still the same as in the 60s to 70s. At 110s, the rotational speed of the system increases steadily and enters a zone of high wind speed. At 130s to 140s, a slight disturbance occurs. If the input is a sine wave, the rotational speed also fluctuates depending on the input. This system looks stable enough when the wind speed is stable or not in a high-speed zone.

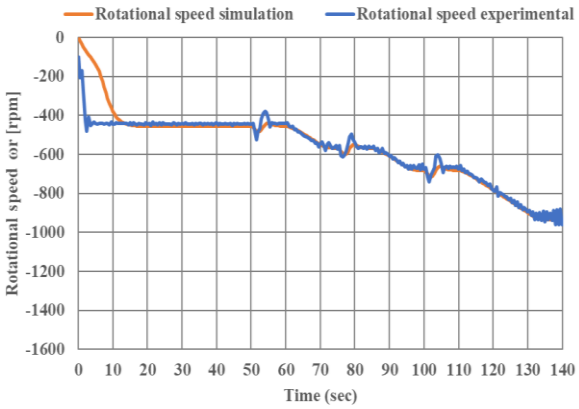

Fig. 16. Rotational speed simulation and Rotational speed experimental.

Table II shows the control parameters of the wind turbine emulator. The pitch angle is used to calculate the wind turbine torque. Coefficient of viscosity for motor, coefficient of viscosity for the wind turbine, moment of inertia for motors, moment of inertia for the wind turbine, and gear ratio are used for inertia modification. Speed gain of analog signals is used to regulate the microcontroller's performance as the data provided contains minor errors in each range of data signals, and the data runs through an electrical circuit, which also amplifies the shift in data sent to the driver. The

microprocessor gain converts the motor torque data to 12-bit data because the digital-to-analog and analog-to-digital functions of the microcontroller use 12-bit memory.

Table III shows the technical data of the servo motor used in this experiment. Table IV shows the specifications of the servo amplifier (servo driver) used in this experiment. The specifications of the servo driver and the servo motor must match for the servo motor to function correctly.

TABLE II: CONTROL PARAMETER OF WIND TURBINE EMULATOR

coefficient of viscosity for motor B_m [Nm/(rad/s)]	0.00095101
coefficient of viscosity for wind turbine B_t [Nm/(rad/s)]	0
moment of inertia for motor J_m [kgm^2]	0.000024610
moment of inertia for wind turbine J_t [kgm^2]	0.104303696
gear ratio n_1/n_2	1
pitch angle[degree]	10
Low-speed gain of analog signal	0.85
Middle-speed gain of analog signal	0.75
High-speed gain of analog signal	0.70
microprocessor gain	3.3/4095

TABLE III: SERVO MOTOR SPECIFICATION

rated output [kW]	0.4
rated torque [Nm]	1.27
max torque [Nm]	3.82
rated speed [rpm]	3000
max speed [rpm]	5000
rated current [A]	2.7
max current [A]	8.1

TABLE IV: SERVO AMPLIFIER SPECIFICATION

voltage input [V]	200-230
phase input	1
phase output	3
voltage output [V]	98
power [kW]	0.4
frequency input [Hz]	50 or 60
frequency output [Hz]	0-333.3
rated current input [A]	4.3
rated current output [A]	2.7

IV. CONCLUSION

This paper proposed the wind turbine emulator for wind power generation system. The wind turbine model is built using the characteristic data of the wind turbine, which is calculated with the lift and drag coefficient to emulate the behavior of the wind turbine when its wind blade is contacted by the neutral wind and generates torque to operate the generator. The wind turbine model is a mathematically calculated model using MATLAB/Simulink. The wind turbine emulator was implemented using a servo motor connected to a small PMSG wind turbine without wind blades. The proposed the wind turbine emulator system has verified its performance by comparing the simulation of the wind turbine model with the results of the experimental system. The wind turbine model contains the wind turbine data and a mechanical model. Therefore, the proposed wind turbine emulator system can test the wind turbine design without actual blades and can be used to analyze various mechanical and electrical characteristics of a PMSG wind turbine connected to the grid.

CONFLICT OF INTEREST

The authors declare no conflict of interest.

AUTHOR CONTRIBUTIONS

S. Reangkittakarn: Conducted the research and wrote the paper, N. Suppaadirek: Conducted the research and analyzed the data and wrote the paper, S. Tammaruckwattana: Analyzed the data and wrote the paper. All authors had approved the final version.

REFERENCES

[1] S. Paul, T. Dey, P. Saha, S. Dey, and R. Sen, "Review on the development scenario of renewable energy in different country," in *Proc. Innovations in Energy Management and Renewable Resource*, Feb. 2021.

[2] A. Parizad and K. J. Hatziadoniu, "Multi-objective optimization of PV/wind/ESS hybrid microgrid system considering reliability and cost indices," in *Proc. of 2019 North American Power Symposium (NAPS)*, Oct. 2019.

[3] F. Chishti, S. Murshid, and B. Singh, "Robust normalized mixed-norm adaptive control scheme for PQ improvement at PCC of a remotely located wind–solar PV-BES microgrid," *IEEE Trans. on Industrial Informatics*, vol. 16, no. 3, pp. 1708–1721, Mar. 2020.

[4] X. Wu, H. Li, X. Wang, and W. Zhao, "Cooperative operation for wind turbines and hydrogen fueling stations with on-site hydrogen production," *IEEE Trans. on Sustainable Energy*, vol. 11, no. 4, pp. 2775–2789, 2020.

[5] M. Hemmati, B. Mohammadi-Ivatloo, M. Abapour, *et al.*, "Optimal chance-constrained scheduling of reconfigurable microgrids considering islanding operation constraints," *IEEE Systems Journal*, vol. 1, no. 4, pp. 5340-5349, 2020.

[6] M. F. A. Fayeem, A. H. Galib, and P. Saha, "Micro wind turbine as an alternative power source in Bangladesh," in *Proc. International Conf. on Sustainable Technologies for Industry 4.0*, Dec. 2019.

[7] D. Li, W. Yang, M. Cai, and J. Wang, "Study of doubly fed induction generator wind turbines for primary frequency control," in *Proc. of IEEE 4th Conf. on Energy Internet and Energy System Integration*, Oct. 2020.

[8] M. Yousefzadeh, S. H. Kia, and D. A. Khaburi, "Emulation of direct-drive wind energy conversion systems based on permanent magnet synchronous generators," in *Proc. 12th Power Electronics, Drive Systems, and Technologies Conference*, Feb. 2021.

[9] A. J. Ferre and O. G. Bellmunt, "Wind turbine generation systems modeling for integration in power systems," in *Handbook of Renewable Energy Technology*, Jan. 2011, pp. 53-68.

[10] K. Ishibashi and H. Yamada, "Modular multilevel converter based single-phase grid-tied wind power generation system with multiple wind power generators under different wind speeds," in *Proc. of 23rd International Conf. on Electrical Machines and Systems*, Dec. 2020.

[11] Y. Ando, N. Yamamura, and M. Ishida, "Maximum power point tracking control method for the small wind power generation system corresponding to wind speed variation," in *Proc. of 23rd International Conf. on Electrical Machines and Systems*, Nov. 2020.

[12] J. Vaheeshan, V. Vihirthanath, S. G. Abeyaratne, A. Atputharajah, and G. Ramatharan. "Wind turbine emulator" in *Proc. of Int. Conf. on Industrial and Information Systems*, 2011, pp. 511-516.

[13] L. D. Danut, N. Muntean, D. Hulea, *et al.*, "Low-cost implementation of a wind turbine emulator," in *Proc. of Int. Conf. on Environment and Electrical Engineering and IEEE Industrial and Commercial Power Systems Europe*, June 2020.

[14] V. T. Ha, V. H. Phuong, N. T. Lam, and N. P. Quang, "A dead-beat current controller-based wind turbine emulator," in *Proc. of International Conference on System Science and Engineering (ICSSE)*, 2017.

[15] A. K. R. Sombra, D. Sgrò, R. P. S. Leao, R. F. Sampaio, and F. C. Sampaio, "Modeling and simulation of an emulator of a wind turbine using vector speed control of a three-phase induction motor," in *Proc. of Simposio Brasileiro de Sistemas Eletricos (SBSE)*, 2018.

[16] E. Mousarezaee, A. Polat and L. T. Ergene, "Wind turbine emulator based on small-scale PMSG by fuzzy FOC," in *Proc. of International Symposium on Electrical Apparatus & Technologies*, 2020.

[17] T. F. dos Santos, I. V. Chacon, G. C. de A. Souza, *et al.*, "Wind Turbine Emulator with DC Motor," in *Proc. of IEEE 15th Brazilian Power Electronics Conference and 5th IEEE Southern Power Electronics Conference (COBEP/SPEC)*, Dec. 2019.

[18] S. Tammaruckwattana and K. Ohyama, "Experimental verification of variable speed wind power generation system using permanent magnet synchronous generator by wind turbine emulator," in *Proc. IECON*, 2012, pp. 5827-5832.

[19] S. Tammaruckwattana, "Modeling and simulation of wind power generation system using diode bridge rectification circuit for converter," in *Proc. of International Conf. on Control, Automation and Systems*, 2015.

[20] S. Tammaruckwattana, "Modeling and simulation of wind power generation system using AC to AC converter," *Lecture Notes in Engineering and Computer Science*, vol. 2, pp. 593-597, 2016.

[21] L. Benaaouinate, M. Khafallah, A. Mesbahi, and A. Martinez, "Development of a useful wind turbine emulator based on permanent magnet DC motor," in *Proc. of International Multi-Conference on Systems, Signals & Devices*, 2017.

[22] M. Yousefzadeh, S. H. Kia, and D. A Khaburi, "Emulation of direct-drive wind energy conversion systems based on permanent magnet synchronous generators," in *Proc. of 12th Power Electronics, Drive Systems, and Technologies Conference*, Feb. 2021.

[23] M. Balaji, S. K. Sarangi, and M. Pattnaik, "Design of a DC motor-based wind turbine emulator using sliding mode control approach," in *Proc. of IEEE 1st International Conf. on Energy, Systems and Information Processing*, July 2019.

[24] N. Suppaadirek, N. Saengsuwan, and S. Tammaruckwattana. "Low wind speed wind turbine blade design for Thailand," *Multidisciplinary Technologies for Industrial Applications*, pp. 29-39, 2020.

[25] A. Mesbahi, M. Khafallah, Y. Aljarhizi, *et al.*, "Boost converter implementation for wind generation system based on a variable speed PMSG," in *Proc. of 1st International Conf. on Innovative Research in Applied Science, Engineering and Technology*, April 2020.

[26] D. H. Wollz, S. A. O. da Silva, and L. P. Sampaio, "Real-time monitoring of an electronic wind turbine emulator based on the dynamic PMSG model using a graphical interface," *Renewable Energy*, vol. 155, pp. 296-308, Aug. 2020.

[27] H. Guo, C. Rui, H. Zeng, and Q. Guo, "Research on the accuracy of large inertia wind turbine emulator," in *Proc. of 22nd International Conference on Electrical Machines and Systems*, Aug. 2019.

[28] Z. Dekali, L. Baghli, and A. Boumediene, "Experimental emulation of a small wind turbine under operating modes using DC motor," in *Proc. of the 4th International Conf. on Power Electronics and their Applications*. Sept. 2019.

[29] R. Nair and G. Narayanan, "Emulation of wind turbine system using vector controlled induction motor drive," *IEEE Trans. on Industry Applications*, vol. 56, no. 4, pp. 4124-4133, July 2020.

[30] P. A. C. Marques, "Digital signal processing education using a low-cost student owned laboratory," in *Proc. of Signal Processing Symposium*, Sept. 2019.

[31] J. Jalden and X. C. Moreno, "Using the Arduino due for teaching digital signal processing," in *Proc. of IEEE International Conference on Acoustics, Speech and Signal Processing*, April 2018.

[32] A. T. Gonzalez, R. P. Gallardo, J. M. Saldana, and G. G. Urueta, "Modeling of a wind turbine with a permanent magnet synchronous generator for real time simulations," in *Proc. of IEEE International Autumn Meeting on Power, Electronics and Computing*, Nov. 2015.

[33] X. C. Fernandez, J. B. Martinez, J. S. Navarro, D. A. A. Roa, L. C. R. Estrada, and M. J. N. Santiago, "Control system design for a 400W micro wind turbine for DC loads applications," in *Proc. of IEEE 9th Annual Computing and Communication Workshop and Conference*, Jan. 2019.

[34] I. Moussa, A. Bouallegue, and A. Khedher, "New wind turbine emulator based on DC machine: hardware implementation using FPGA board for an open-loop operation," *IET Circuits, Devices Systems*, vol. 13, no. 6, pp. 896–902, May 2019.

[35] E. Lerma, R. Costa-Castello, and R. Grino. "Duino-based learning (DBL) in control engineering courses," in *Proc. of IEEE International Conf. on Emerging Technologies and Factory Automation*, Sept. 2019.

[36] N. Vijayan, J. Sandeep, and R. Ramchand, "An Arduino based speed and rotor position measurement technique for electric drives," in *Proc. of International Conf. on Power Electronics Applications and Technology in Present Energy Scenario*, Aug. 2019.

[37] I. Moussa and A. Khedher, "Real-time WTE using FLC Implementation on FPGA board: Theoretical and Experimental Studies," in *Proc. of 17th International Multi-Conference on Systems, Signals & Devices*, July 2020.

[38] F. O. S. Gama, J. K. E. da C. Martins, T. F. de Miranda, W. M. de F. Tome, S. N. Silva, and M. A. C. Fernandes, "Control of airflow in ventilation systems using embedded systems on microcontrollers," in *Microsystem Technologies*, March 2019, pp. 4067-4076.

[39] MATLAB/Simulink license for King Mongkut's Institute of Technology Ladkrabang, license Number: 40904942

Natchanon Suppaadirek (Member) received the B.E. degree in Mechatronics Engineering from King Mongkut's Institute of Technology Ladkrabang, Bangkok, Thailand, in 2019. In August 2019, he studied M.E. degree in Control Engineering from King Mongkut's Institute of Technology Ladkrabang, Bangkok, Thailand. His current research interests include Wind Turbine Emulator.

Sitthaphat Ruengkittrakarn (Member) received the B.E. and M.E. degrees in Instrumentation Engineering from King Mongkut's Institute of Technology Ladkrabang, Bangkok, Thailand, in 2001 and 2005, respectively. His current research interests include variable speed wind power generation systems using diode bridge rectifier circuits with the wind turbine.

Sirichai Tammaruckwattana (Member) received the B.E. and M.E. degrees in Electrical and Control Engineering from King Mongkut's Institute of Technology Ladkrabang, Bangkok, Thailand, and D.Eng. degree in Material Science and Production Engineering from Fukuoka Institute of Technology, Fukuoka, Japan, in 2001, 2005, and 2015, respectively. In December 2005, he joined the Department of Instrumentation and Control Engineering, King Mongkut's Institute of Technology Ladkrabang, Bangkok, Thailand, as a Lecturer. In November 2016, he was promoted to Assistant Professor in the department. His current research interests include wind power generation systems.